Åbo Akademi

OPEN ACCESS

This is an electronic reprint of the original article. This reprint may differ from the original in pagination and typographic detail.

Hydrogen production from sucrose via aqueous-phase reforming

Godina, Lidia; Heeres, Hans; Garcia, Sonia; Bennett, Steve; Poulston, Stephen; Murzin, Dmitry

Published in:
International Journal of Hydrogen Energy

DOI:
10.1016/j.ijhydene.2019.04.123

Published: 01/01/2019

Document Version
Accepted author manuscript

Document License
CC BY-NC-ND

Link to publication

Please cite the original version:
Godina, L., Heeres, H., Garcia, S., Bennett, S., Poulston, S., & Murzin, D. (2019). Hydrogen production from sucrose via aqueous-phase reforming. *International Journal of Hydrogen Energy*, *44*(29), 14605–14623. https://doi.org/10.1016/j.ijhydene.2019.04.123

General rights
Copyright and moral rights for the publications made accessible in the public portal are retained by the authors and/or other copyright owners and it is a condition of accessing publications that users recognise and abide by the legal requirements associated with these rights.

Take down policy
If you believe that this document breaches copyright please contact us providing details, and we will remove access to the work immediately and investigate your claim.

This document is downloaded from the Research Information Portal of ÅAU: 13. Mar. 2024

Hydrogen production from sucrose via aqueous-phase reforming

Lidia I. Godina[a], Hans Heeres[b], Sonia Garcia[c], Steve Bennett[c], Stephen Poulston[c], Dmitry Yu. Murzin*[a]

* - corresponding author: dmurzin@abo.fi

[a] - Laboratory of Industrial Chemistry and Reaction Engineering, Process Chemistry Centre, Åbo Akademi University, FI-20500 Turku/Åbo, Finland

[b] - Biomass Technology Group BV, Josink Esweg 34, 7545 PN Enschede, the Netherlands

[c] - Johnson Matthey Technology Centre, Sonning Common, Reading RG4 9NH, United Kingdom

Abstract

Commercial sucrose was used to produce hydrogen in a combined approach of hydrogenation and aqueous phase reforming (APR). First a mixture of technical sorbitol/ mannitol was produced by hydrogenating an aqueous solution of sucrose in a trickle bed reactor over 5 wt % Ru/C. The produced polyols were treated in a continuous reactor at 498 K and elevated pressure deploying a 2.5 wt % Pt/C catalyst to yield hydrogen. The highest hydrogen selectivity was 62%. No large differences were found when comparing a commercial available sorbitol to the technical sorbitol/mannitol mixture in terms of conversion levels and selectivity to the gas-phase products. This was accompanied by a similar distribution of products retained in the liquid phase. The efficiency of APR when utilizing Pt/C was found to be still insufficient for industrial implementation in terms of hydrogen production. Thus, additional efforts should be made to increase the obtained amounts of hydrogen per mole of converted sugar alcohols.

Keywords: aqueous-phase reforming, sucrose hydrogenation, sorbitol, mannitol, technical feed, platinum, hydrogen

Highlights:

- For the first time a hydrogenated sucrose solution was compared to a commercial sorbitol in APR over Pt/C catalyst for hydrogen generation
- A similar selectivity towards the main gaseous products (hydrogen, carbon dioxide, and alkanes) was obtained
- A minor difference between liquid-phase products and catalysts activity was observed
- Characterization of Pt/C by temperature programmed oxidation is useful for quantification of light products
- Pt/C catalysts displayed low efficiency in terms of hydrogen production
- Application of Pt/C requires efficient removal of hydrogen, low hydrogen pressure or operation under low conversion levels

1. Introduction

Biomass, and especially carbohydrates obtained from starch-rich and cellulosic materials, can become a dominant feedstock for the sustainable production of fuels, chemicals and materials according to Lynd et al. [1]. The current existing technologies for the production of first generation biofuel, e.g. biomass-to-ethanol processes, are developed for the utilization of fermentable sugars mainly obtained from sugarcane and starch rich crops. A second generation feedstock, lignocellulosic biomass (e.g. agricultural residues, wood, etc.), is much more complex. It contains cellulose and hemicelluloses as a source of carbohydrates in a complex matrix, comprising also lignin. Due to this complexity, liberating sugars from lignocellulosic biomass is a more demanding process compared to the starch rich feeds, requiring a multiple pretreatment approach [2].

Carbohydrates can be utilized in various processes to produce fuels and chemicals. One of the approaches is to apply aqueous-phase reforming (APR), allowing production of hydrogen and alkanes at relatively low temperatures and pressures. In APR, the conversion of an aqueous solution of a certain substrate is performed over a heterogeneous catalyst at typically 463-523 K and 25-60 bar [3] to maintain the liquid phase. Various transition metals in combination with various supports can be applied as catalysts in APR. However, this reaction requires catalysts having a high hydrothermal stability and resistance towards impurities present in the feedstock.

The APR of aqueous solutions of model compounds and various lignocellulosic biomass has been studied in detail and described in the literature by various research groups. The majority of studies reported in the literature are devoted to investigation of APR of model compounds, such as neat alcohols and polyols ranging from C1 to C6. Methanol, ethylene glycol, glycerol, xylitol and sorbitol are often applied as a feed [4–

7]. The difference between polyols with the different carbon chain length was demonstrated in [8,9]. An increase in the carbon chain length gives better selectivity to higher alkanes and leads to a decrease in hydrogen selectivity.

Sugar solutions (fructose, glucose, sucrose) were tested over transition metal catalysts, such as Ni/Al_2O_3, Ni/Ce_2O-Al_2O_3, Ni/ZrO_2, Pd/Al_2O_3, Pt-Ni/Al_2O_3, Pt/Al_2O_3, Pt/Ce_2O-Al_2O_3, Pt/ZrO_2 [10]. Coke formation was identified as the main reason for catalyst deactivation. Glucose APR was studied over doped graphene [11], Pt/C [12,13], Pt/Al_2O_3 [8,14,15]. Severe degradation of glucose through side reactions was also detected over Ni/Al_2O_3 [16]. Comparably low selectivity to hydrogen was obtained during the glucose APR over carbon-supported transition metals (Pt, Pt-Ni, Pt-Ru, Pt-Sn, Pt-Ni-Sn) [17]. Lactose APR was investigated over Ni-La/Al_2O_3, Ni-Co/Al_2O_3-MgO, and Ni-La/Al_2O_3 catalysts [18,19] and an overlayer of Pt on Ni or Co on Pt [20]. Several attempts were made for direct biomass gasification and utilization of various biomass with minimal pretreatments, examples of which including such feedstock, as wood, cellulose, lignin and its monomers, hydrolysate of lignocellulosic biomass, are discussed below.

Batch-wise direct wood gasification was performed via combination of acid hydrolysis and APR over Pt/Al_2O_3 [15]. Pine sawdust and waste paper were found to be similar to glucose and ethylene glycol in terms of hydrogen production per mass of feed. More acidic conditions promoted hydrogen production due to more effective hydrolysis of polysaccharides.

Screening of carbon supports was performed for APR of wheat straw hydrolysate over Pt/C catalysts [21]. Various carbon supports were tested, such as activated carbon (AC), graphene oxide (GO), multi-walled carbon nanotubes (MWCNT), super-Darco carbon (SDC), and single-walled carbon nanotubes (SWCNT). The best performance was

obtained with activated carbon and SWCNT, which can be mainly related mainly due to the large size of the polysaccharide molecules not being able to reach Pt sites located inside graphene layers. Bimetallic and trimetallic catalysts were compared in terms of activity and selectivity towards hydrogen in the conversion of glucose and wheat straw hydrolysate APR [17] using the following metals and metal combinations with AC and MWCNT as supports: Pt, Pt-Ni, Pt-Ru, Pt-Sn, Pt-Ni-Sn. Wheat straw hydrolysate was more selective to hydrogen compared to glucose and Pt-Ru/AC, Pt-Ni/AC and Pt-Ru/MWCNT appeared to be the best candidates for hydrogen production among all tested catalysts. APR of kenaf hydrolysate was performed over Pt/C [22], Pt/Al_2O_3 and Ru/C [23]. Higher hydrogen production was obtained in the experiment with the hydrogenated kenaf hydrolysate compared to glucose and the non-hydrogenated hydrolysate. Optimum conditions were determined for the APR of sorghum hydrolyzate over Raney-Ni [24].

Direct conversion of cellulose arouses interest of many researchers as it can eliminate the need for initial hydrolysis. The degree of crystallinity was found to be crucial for hydrogen production via APR of various sources of cellulose (filter paper, degreased cotton, microcrystalline cellulose) over Pt/C [13]. At the same time, hydrogen selectivity and yield were much lower in the case of glucose APR. According to the same study, platinum appeared to be the best metal for cellulose conversion among the studied metals (Pt, Pd, Ni, Co and Ir). Cellulose conversion to hydrogen appeared to be slightly more efficient over Pt/Al_2O_3 than over Pt and Pt-Ru catalysts supported on carbon textile [25]. One pot conversion of cellulose via polyols to hydrogen by APR was studied over Pt/Na(H)ZSM-5 [26]. Pt/C catalyst was compared to a powdered tungsten and tungsten coated oxidized Si wafers prepared by magnetron sputtering of tungsten coating in the cellulose APR [27]. Sputtered tungsten catalyst was stable in

the presence of sulphur- and nitrogen-containing compounds, being 10-fold more active compared to Pt/C. Nickel catalysts supported on layered double oxides were found to be efficient and stable for the conversion of cellulose to hydrogen [28].

APR of lignin and several monomers (catechol, guaiacol, methanol, phenol, syringol) was performed over Pt/ZrO_2, Pt/Al_2O_3, Pt/C, Pt/TiO_2, and Ni/C in order to propose the corresponding reaction network [29], while phenol was tested over Ni/ZSM-5 [30,31]. Besides lignocellulosic biomass, alginate APR was conducted over Pt/C focusing on the influence of operation parameters [32].

Byproducts of pyrolytic bio-oil production, such as an aqueous phase and low boiling fractions of pyrolysis oil, were also tested in APR. This type of feed has a large potential, since the produced hydrogen can be utilized on-site for bio-oil upgrading. An aqueous fraction of pyrolytic bio-oil was applied in APR over Pt/Al_2O_3 [33]. APR was performed with a not treated and hydrogenated. The hydrogen selectivity obtained by applying the hydrogenated feed gave results similar to the values observed during the sorbitol APR. The distillate of crude bio-oil was converted over Pt/Al_2O_3 [34,35] and Pt/CeO_2-TiO_2 and Pt/CeO_2-ZrO_2 catalysts [35]. Mixed zirconia-ceria and ceria-titania oxides were as selective to hydrogen as alumina displaying higher hydrothermal stability. Influence of temperature and concentration on the APR of the low-boiling fraction of rice husk pyrolyzed bio-oil was investigated over Pt/Al_2O_3 [36].

APR of crude glycerol was studied over Ni/SiO_2-Al_2O_3 focusing on the feed concentration, temperature and the role of impurities [37]. A pronounced inhibition effect on hydrogen production was shown in the crude glycerol APR over Pt supported on alumina, carbon and magnesium aluminate due to formation of long chain olefins and aliphatics from sodium salts of fatty acids [38]. The role of operating conditions was thoroughly studied in the crude glycerol APR over Ni-La/Al_2O_3 catalyst [39].

The APR of waste lipids with formation of linear hydrocarbons was performed over Pt-Re/C [40].

Slightly more exotic examples are the APR of cheese whey [18,19], fermentation broth [41], and tuna-cooking waste water [42]. Optimum parameters were proposed for cheese whey valorization via APR over Ni-La/Al_2O_3, Ni-Co/Al_2O_3-MgO, and Ni-La/Al_2O_3 [18,19]. Biomass hydrolysate usually contains relatively large polysaccharides, therefore certain mass-transfer limitations can take place during degradation of this feed [17]. Thus, certain unsolved problems are associated with the direct reforming of biomass. The overall conclusion from studies on sugar APR is that sugars appeared to be a problematic feed due to high coke formation rates and subsequently fast catalyst deactivation. An additional step – hydrogenation of sugars – should be applied to diminish coke formation and to increase the total hydrogen production by increasing the degree of feed utilization [23]. Hydrogenated glucose solution was studied previously [23], however, the catalyst behaviour with time on stream was not discussed. This topic was considered in the current study for the first time.

In this work model compounds and technical feeds were tested and compared in APR over Pt/C catalyst at 498 K and 29.7 bar. Important parameters in this investigation were: catalyst activity, selectivity and the yield of gas- and liquid-phase products. Commercial sorbitol represented the model compound, and the technical feed was a mixture of polyols obtained from a hydrogenated aqueous sucrose solution. Long-term stability tests were performed (120 and 160 h time-on-stream) to elucidate potential catalyst deactivation. Additional supporting studies were performed in a batch reactor. Hydrogen production per mole of converted sorbitol was compared for various

alumina- and carbon-supported catalysts described in the literature and the current study.

2. Experimental

2.1. Materials

Platinum catalyst containing 2.5 wt % of the metal supported on activated carbon (Pt/AC-JM) was provided by Johnson Matthey.

Additionally, two Pt catalysts were prepared via incipient-wetness impregnation of an activated carbon support. Commercial activated carbon from Merck (AC-MkU) was crushed and sieved prior to impregnation to the following fractions: 1.0-2.0 mm (Pt/AC-4) and <0.1 mm (Pt/AC-1). A solution of $H_2Pt(NO_3)_6$ in aqueous HNO_3 was used as a precursor. Catalysts were treated with air flow in an oven at 373 K during 2 hours, reduced at 523 K, and passivated. Metal content was targeted to be 2.5 wt %.

The Ru/C (5 wt %) used was purchased from KaiDa, Shaanxi, China.

The (beet) sucrose was a food grade sugar purchased from a food market in the Netherlands.

Commercial sorbitol (≥98%) was provided by Sigma-Aldrich.

2.2. Catalysts characterization

Textural properties of the Pt/AC-JM catalyst were studied by nitrogen physisorption on a gas sorption system Autosorb iQ/ASiQwin (Quatachrome instruments).

The reduction temperature of Pt/AC-JM was identified by means of temperature programmed reduction (TPR) performed in an AutoChem 2900 instrument. The catalyst sample (0.1 g) was reduced in a U-shaped quartz tube in 5% H_2/Ar flow. The sample was heated from room temperature to 973K at a rate of 5K/min. Subsequently

the hydrogen uptake was measured by a thermal conductivity detector (TCD). Gas effluent passed through a cold trap (liquid nitrogen and isopropanol syrup, 185 K) to exclude the influence of water on the signal. Additionally, a mass spectrometry (MS) detector was applied without the cold trap for identification of the gas-phase composition.

Temperature-programmed desorption (TPD) of ammonia was applied for studying the Pt/AC-JM catalyst acidity by means of pulse chemisorption apparatus (Micromeritics, AutoChem 2900). The catalyst was dried at 373 K overnight prior to analysis. The sample (0.1 g) was loaded in a quartz U-tube and reduced in an excess of hydrogen (flow: 20 mL/min STP) at 548 K (heating rate 5 K/min) during 2 hours. Hydrogen was removed by flushing with He (20 mL/min STP, 30 min); thereafter the reduced sample was cooled down to the ambient temperature. Ammonia treatment with 5 % NH_3 in He was performed during 1 h. Physically adsorbed ammonia was removed by He flow (20 mL/min STP, 30 min). The sample was heated to 498 K or 673 K with different heating rates (3, 5, 10, 15, 20 K/min). After each heating step the sample was cooled to ambient temperature, flushed with He (20 mL/min STP, 15 min), and saturated with ammonia as described above.

The heat of desorption was calculated using a conventional approach plotting $1/T_p$ against $\ln(T^2/b)$, where T_p is the temperature of the maximum desorption and b is heating rate, determined as the slope [43].

The platinum dispersion was evaluated for fresh Pt/AC-JM catalysts by CO pulse chemisorption (Micromeritics, AutoChem 2900). The following program was used for the catalyst pretreatment prior to analysis: heating from 298 to 323 K at 10 K/min in He, dwelling for 30 min, gas switch to H_2, heating to 523 K at a rate of 5 K/min, dwelling for 2 h, followed by a flushing for 60 min in He. In the first step the sample

(0.1 g) was pre-reduced in a U-shaped quartz tube, while in the second step the surface hydrogen was removed. After this procedure the catalyst was cooled to ambient temperature and titrated by CO pulses (10 vol % CO in He). The Pt/CO stoichiometry was assumed to be 1/1. A similar procedure was applied for the fresh Pt/AC-1, Pt/AC-4 catalysts in a chemisorption apparatus (Micromeritics, AutoChem II). During the pretreatment stage the catalyst samples (0.1 g) were flushed with 5% H_2/N_2, heated up to 523 K with applying a heating rate of 10 K/min. After the reduction, which lasted for 10 minutes, the samples were cooled down to 303 K and flushed with He. During chemisorption pulses of CO were fed with the flow rate 30 mL/min together with He (50 mL/min STP). Helium was applied as a carrier-gas.

Spent Pt/AC-1 and Pt/AC-4 catalysts were washed with deionized water and dried over night at room temperature. Complete removal of water was achieved during the final drying in a vacuum oven overnight at 313 K.

Thermo-gravimetric analysis (TGA) in air was performed for the fresh and spent Pt/AC-1 and Pt/AC-4 catalysts (each probe is 16-24 mg) with SDT Q600 V8.3 thermal analyzing instrument at 100 mL/min (STP) air flow and heating rate 5 K/min up to 1173 K. Heat flows were measured by differential scanning calorimetry (DSC). All spent catalysts, except for one, were thoroughly washed with 200-300 mL of deionized water to remove absorbed polyols and water-soluble reaction products from the catalyst.

The metal content in the fresh and spent Pt/AC-1 and Pt/AC-4 catalysts was determined by ICP.

The size and the structure of metal particles of the Pt/AC-JM catalyst was studied by transmission electron microscopy (TEM) on a JEM-2010 microscope (JEOL, Japan) with a lattice resolution of 0.14 nm at an accelerating voltage of 200 kV.

2.3. Preparation of technical sorbitol-mannitol mixture

Large quantities of technical mixed polyols (+15 kg) were produced by hydrogenation of an aqueous sucrose solution (50 wt %) in a trickle bed reactor over 5 wt % Ru/C catalyst at 453 K and 50 bar. The reactor scheme can be found in Figure S1 (Supporting information). The sucrose solution was fed with a flow rate of 80 g/h (corresponding WHSV was equal to 2 h^{-1}). Hydrogen flow was 60 L/h (STP). The produced polyol feed was diluted to 29 wt % to prevent the blockage of the feed pump and/or reactor inlet by crystallization of mannitol during the longer term processing (as observed in preliminary experiments). The details of hydrogenation can be found in the Supporting information.

2.4. Aqueous-phase reforming of technical sorbitol-mannitol mixture

Aqueous-phase reforming of the technical polyol solution was performed in continuous and batch mode. The Pt/AC-JM catalyst was only utilized in the continuous set-up to process the technical feed and commercial sorbitol. The Pt/AC-1 and Pt/AC-4 catalysts were applied in the batch reactor with the technical feed.

2.4.1. Continuous reactor

The details on the experimental set-up can be found in an earlier publication [44]. The catalyst (0.5 g, powder) was mixed with quartz sand (1 g, mesh size 200-800 μm) to minimize the pressure drop. The catalyst layer was located in-between two layers of sand in the middle of a stainless-steel reactor tube, which was placed in a furnace. Experiments were performed in a downflow concurrent mode. The catalyst was reduced *in situ* prior to the experiments during 2 hours at 573 K applying hydrogen (40 mL/min, STP). Residual hydrogen was removed by flushing with N_2 (25 mL/min, STP) for 20

min; the reactor was subsequently pressurized to the desired reaction pressure with nitrogen containing 1% He, and heated to 498 K. An HPLC pump was used for feeding the aqueous solution of sorbitol (0.27 mol/L, or 4.9 wt %) or the mixture of technical polyols (0.26 mol/L, or 4.6 wt %). The density of the polyol solutions was determined according to [45] and used to calculate the polyol concentration (wt %). The liquid flow rates varied from 0.1 to 1 mL/min, which corresponds to weight-hour space velocities of 0.5-1.1 h^{-1} calculated as mass of the substrate per mass of the catalyst per hour (g x g^{-1} x h^{-1}). A constant co-feeding of N_2 (1% He) carrier gas (19 mL/min, STP) was applied to maintain the pressure inside the reactor. Helium was utilized as an internal standard for GC analysis.

The liquid samples were taken via a sampling loop at the bottom of the reactor. Analysis of the liquid phase products was performed by HPLC. The same procedure was applied for the analysis of the initial technical feed (Aminex HPX-87H, RI detector, 45°C, 5 mM H_2SO_4, isocratic conditions, 0.6 mL/min).

The gas samples were analyzed online by a Micro-GC (Agilent Micro-GC 3000A) equipped with four columns: Plot U, OV-1, Alumina and Molsieve.

The carbon balance was elucidated by total organic carbon analysis.

A list of experiments performed in the continuous set-up is given in Table 1. Pt/AC-JM catalyst was applied in the APR of sorbitol at 29.7 bar during 161 hours, then the pressure was increased to 40 bar and the experiment at the elevated pressure and 498 K continued for 24 hours. Elevation of pressure was performed to check experimentally if there was too excessive evaporation of water at lower pressure influencing the catalytic results or if a higher hydrogen pressure can adversely affect conversion and selectivity. Because of minor differences in conversion and selectivity, results of this experiment will not be further discussed in this contribution focused on APR of a

technical feed. The catalyst was subsequently reactivated in the following manner: the reactor was cooled down to 308 K, depressurized, the catalyst was flushed with deionized water (2.0 mL/min, 10 min), acetone (2.0 mL/min, 10 min), and again with water (2.0 mL/min, 10 min). Acetone flushing was applied to remove water-insoluble compounds. The catalyst was then heated to 573 K (heating rate 5K/min) for a subsequent reduction in the hydrogen (40 mL/min, STP) for 2 hours. After the regeneration step, the catalyst was cooled down to the reaction temperature (498 K), and the diluted aqueous solution of technical polyols was introduced. The APR with the diluted feed lasted for 120 hours. The experiment with the concentrated solution of polyols (29 wt %) was performed over a fresh sample of Pt/AC-JM.

Table 1. Experiments in the continuous set-up.

Step	***Polyol content, [wt %]***	***Pressure, [bar]***	***TOS, [h]***	***Catalyst loading***	***Reduction temperature, [K]***
APR of sorbitol	4.9	29.7	161	Fresh	573
APR of sorbitol	4.9	40	24	Same	-
APR of technical feed	4.6	29.7	120	Same regenerated	573
APR of technical feed	29	29.7	145	Fresh	-

2.4.2. Batch reactor

APR of the technical feed was performed in an autoclave (300 mL), made from Hasteloy. The autoclave is equipped with a heating/cooling jacket, gas inlet and outlet, and an internal thermocouple. A conventional propeller stirrer was applied for an experiment with the powder catalyst Pt/AC-1 and a blank test, while a cage reactor was

used for the experiment with the Pt/AC-4 catalyst (granule size 1-2 mm). The cage reactor is made from two perforated cylinders assembled together with two round holders, in a way that the space in between these cylinders could be filled with the catalyst. Water was continuously circulated through this system, being sucked by built-in impellers from the top and bottom holes, and coming out from the holes of the external cylinder (average hole diameter is 0.9 mm).

Catalytic tests were performed at 498 K and at 30 bar initial N_2 pressure, with a stirring rate set at 1000 rpm. The feed and the catalyst were loaded, and the reactor was closed and flushed 10 times with nitrogen. An external cylinder for gas collection was attached to the system. After pressurizing to 30 bar and sealing, the reactor heating was started with a heating rate 5 K/min. The stirring (200 rpm) started at the same moment. The zero-time of the reaction was taken at the moment when temperature reached 498 K and the stirring rate was increased to 1000 rpm. The reaction was stopped after 2 hours by reducing the stirring rate to 200 rpm and cooling the reactor down with cold tap water. Gas and liquid samples were taken when the reactor temperature reached 293-303 K.

The experiments performed in the batch reactor are listed in Table 2. The blank experiment and the experiment with the Pt/AC-1 powder were performed with a ~15.3 wt % polyol solution, while a more diluted feed (~4.0-5.6 wt %) was applied with the Pt/AC-4 catalyst. Three experiments with the same Pt/AC-4 sample were performed in order to study catalyst deactivation. Additional long-term studies (up to 24 h) were performed with the same catalyst.

Table 2. Experiments in the autoclave.

Catalyst	*Support size, [mm]*	*Catalyst weight, [g]*	*Polyol content, [wt %]*	*Duration, [h]*	*Stirrer*
blank	-	-	15.3	2	impeller
Pt/AC-1	<0.1 mm	6	15.3	2	impeller
Pt/AC-4	1.0-2.0	2.9	5.6	2 x 3	cage
Pt/AC-4	1.0-2.0	2.32	4.6	1	cage
Pt/AC-4	1.0-2.0	2.02	4.1	2	cage
Pt/AC-4	1.0-2.0	2.12	4.1	4	cage
Pt/AC-4	1.0-2.0	2.02	4.1	8	cage
Pt/AC-4	1.0-2.0	2.02	4.0	24	cage

Analysis of the liquid phase products were performed by HPLC. The same procedure was applied as for the analysis of the initial feed (Aminex HPX-87H, RI detector, 45°C, 5 mM H_2SO_4, isocratic conditions, 0.6 mL/min). The carbon content in the initial feed and in the produced liquid phase was determined by CHN analysis

The gas samples were analysed by an Agilent Technologies 7890A instrument equipped with JW CP8713 column and TCD detector. The column was calibrated prior to analysis with a mixture of H_2, N_2, CO, CO_2, C_3H_6 and light alkanes C_1-C_4.

2.5. Equations

The following equations were applied. Conversion was calculated as:

$$Conversion\ (\%) = \frac{C_{pol\,in} - C_{pol\,out}}{C_{pol\,in}} \cdot 100\% \,, \qquad (1)$$

where $C_{pol\,in}$ – input polyol concentration [mol/L], $C_{pol\,out}$ – output polyol concentration [mol/L].

The carbon conversion to the gas phase was defined in the following way:

$$Carbon\ conversion\ (\%) = \frac{\nu(CC_{gas})}{\nu(CC_{pol\,in})} \cdot 100\% \,, \qquad (2)$$

where $\upsilon(CC_{gas})$ – the total amount of carbon in all gas-phase products (CO_2, CO and alkanes) or the corresponding molar carbon flow [mol C or mol C/min], $\upsilon(CC_{pol\,in})$ – the amount of carbon in the input polyol or the corresponding molar carbon flow [mol C or mol C/min].

The selectivity to alkanes, CO_2 and CO was defined as:

$$Selectivity\ to\ product\ X(\%) = \frac{\upsilon(CC_X)}{\upsilon(CC_{gas})} \cdot 100\%\ , \quad (3)$$

where $\upsilon(CC_x)$ – carbon, contained in a product X, or the corresponding carbon flow [mol C or mol C/min].

The yield of the liquid-phase products was defined as:

$$Yield\ of\ product\ X(\%) = \frac{\upsilon(CC_X)}{\upsilon(CC_{pol\,in})} \cdot 100\%\ , \quad (4)$$

Selectivity to hydrogen is defined in the following way:

$$Selectivity\ to\ H_2(\%) = \frac{\upsilon(C_{H2})}{\upsilon(CC_{gas})} \cdot \frac{1}{RR} \cdot 100\%\ , \quad (5)$$

where $\upsilon(H_2)$ – the amount of H_2 formed, or the corresponding flow rate [mol or mol/min], and reforming ratio *RR*=13/7 for sorbitol and mannitol. The reforming ratio *RR* (H_2/CO_2) was introduced to calculate the selectivity to hydrogen, since hydrogen is produced both from polyol and via the water-gas shift (WGS) reaction:

$C_6H_{14}O_6 \longrightarrow 6CO + 7H_2 \xrightarrow{+6H_2O} 6CO_2 + 13H_2$

The molar flow of carbon $\nu(CC_X)$ is determined as:

$$\nu(CC_X) = C_X \cdot \nu \cdot n, \quad (6)$$

where C_x – concentration of a substance X [mol/L]; υ – volumetric flow [L/min]; n – number of carbon atoms in the substance X.

3. Results and Discussion

3.1. Catalysts characterization

The Pt/AC-JM catalyst has a specific surface area of 963 m^2/g, pore volume 0.83 cm^3/g, and the average pore diameter of 6.3 nm, determined by the Barrett-Joyner-Halenda method. The activated carbon (Merck AC-MkU) applied as a support for Pt/AC-1 and Pt/AC-4 has a specific surface area of 927 m^2/g.

The reduction curve of the Pt/AC-JM catalyst is presented in Figure S2 in the Supporting information. The curve was obtained during the TPR performed with the cold trap (185 K) to remove water from the gas phase. Two local minima at 314 and 500 K correspond to the reduction of Pt. However, the TPR curve reflects not only the hydrogen consumption, but also the formation of CH_4 and CO, which was confirmed by MS analysis (Figure S3). It is known that functional groups on the carbon surface can be decarbonylated, decarboxylated or reduced over Pt during TPR [46,47]. In the current study, CO formation started at temperatures exceeding 484 K. A small amount of methane was formed below 588 K, and it accelerated after 778K. CO_2 was not detected, being probably reduced to CO.

Acidity of Pt/AC-JM catalyst was determined by ammonia desorption; the curves and determination of the ammonia desorption energy can be found in Figure S4, Supporting info. The ammonia desorption energy E_{des} was equal to 40 kJ/mol. The amount of acid sites was 42 μmol NH_3/g catalyst. This data is consistent with the previous studies on similar carbon-supported catalysts [43,44].

The metal particle size of the fresh Pt/AC-JM catalyst, determined by CO-chemisorption (22.6 nm, 5% dispersion) is in a clear disagreement with the TEM analysis of a fresh sample (average size of 1.7 nm). This inconsistency can be explained

by the presence of metal agglomerates in the spent catalyst sample (Figure 1). The fresh Pt/AC-1 and Pt/AC-4 catalysts showed similar particle diameters of 8.0 and 8.1 nm and a moderate dispersion of 14% (determined by CO-chemisorption).

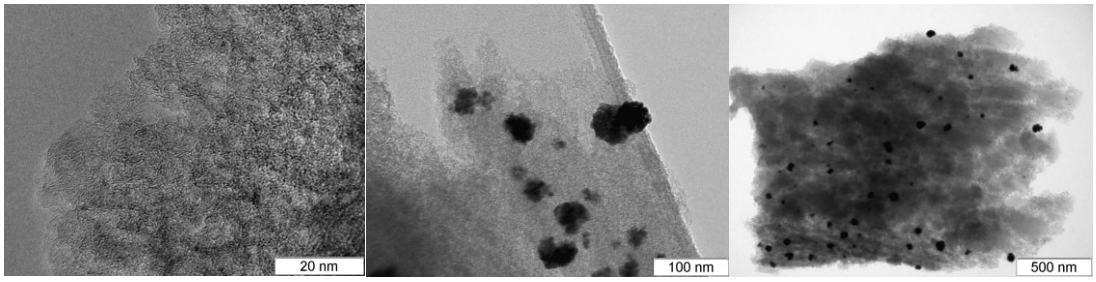

Figure 1. TEM images of the spent Pt/AC-JM sample.

The Pt/AC-JM catalyst was mixed with quartz sand for the experiment in the continuous mode, which appeared to be a challenge for subsequent analysis of the spent catalyst properties due to difficulties of catalyst separation from the quartz sand.

Textural properties of the activated carbon support from Merck, which was utilized for preparation of Pt/AC-1 and Pt/AC-4, can be found in [48].

The TGA/DTG/DSC plots of the Pt/AC-1 are shown in Figure 2 (upper three) for the fresh, spent but not washed, and washed samples. The three lower plots in Figure 2 represent TG analysis of the Pt/AC-4: the fresh and two spent samples (2 hours and 2x3 hours in the batch).

Both Pt/AC-1 and Pt/AC-4 catalysts underwent a substantial mass loss (12-15%) at temperatures 613-663 and 573-630 K correspondingly, as can be seen from Figure 2. This can be attributed to the loss of the weakest surface groups through decarboxylation [49]. The Pt/AC-1 exhibited another sharp mass loss (28%) at 745 K, while Pt/AC-4 was slowly oxidized in a temperature range from 627 to 813 K with a 20% mass loss.

The final period of carbon support burning appeared at 733-863 K (Pt/AC-1, 49%) and 813-893 K (Pt/AC-4, 59% mass loss), when the support was burnt completely.

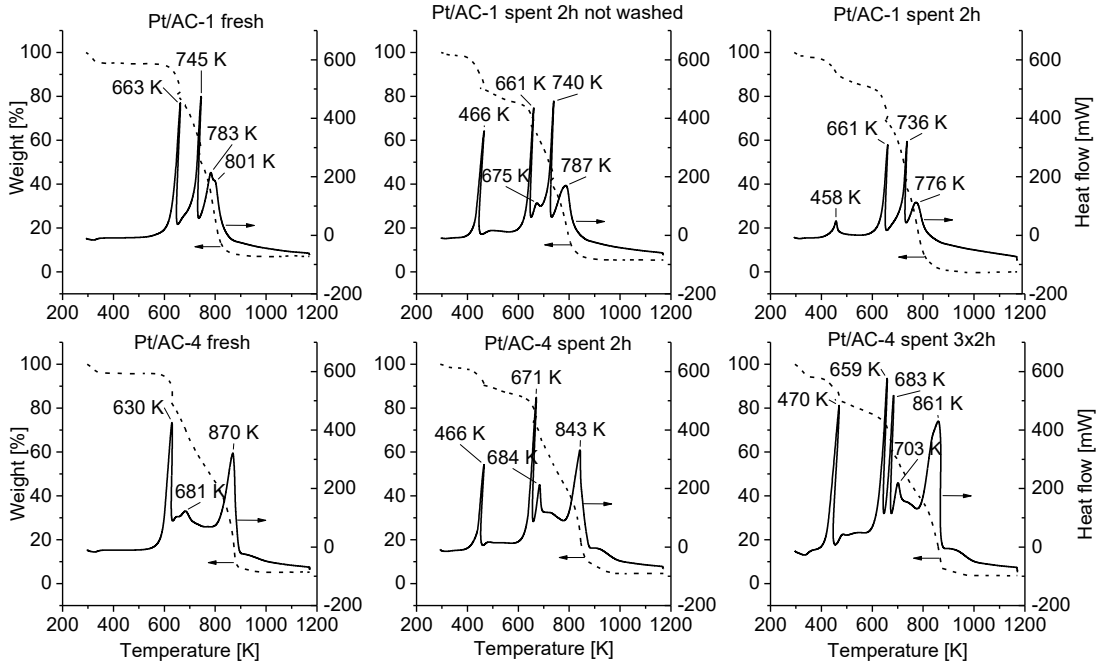

Figure 2. TGA of fresh and spent Pt/AC-1 (upper row) and Pt/AC-4 (lower row) catalysts. Weight and heat flow are shown as a function of temperature.

The spent catalysts showed highly exothermic mass losses (3-15%) at 393-466 K. This can be attributed to a catalytic oxidation of feed and products present in the catalyst pores rather than to the feed oxidation, which occurred at 623 and 638 K for sorbitol and mannitol correspondingly [50–52]. Another additional exothermic mass loss in the spent catalysts occurred at 663-673 K, which is much more challenging to explain due to complexity of the processes taking place during TPO analysis. Similar mass losses at 400-460 K and 663-673 K were obtained for a spent Pt/Al_2O_3 catalyst utilized in sorbitol APR [53,54].

Activated carbons are in general not very stable at temperatures above 673 K. Autoignition of activated carbon occurs during treatment with hot air at 725 K [55]. The losses of surface groups (573-673 K) and subsequent carbon skeleton decomposition (above 673 K) were detected during TPO of activated carbon prepared from Babassu palm petiole [49]. In addition, it was shown that Vulcan carbon black is significantly more thermally stable than the corresponding Pt/C impregnated catalyst with high metal loadings (20-46 wt %) [56–59]. Similar results were obtained for the Pt/C catalyst (1-2 wt %), supported on activated carbon [60]. The expected temperature of coke burning is above 873 K [61]. According to the facts mentioned above, TPO/DSC cannot be considered as an effective method for investigating coke formation on Pt/AC due to low stability of the support. However, it could be applied for an approximate estimation of absorbed initial feed and products from the liquid phase.

The Pt content of the fresh and spent Pt/AC-1 and Pt/AC-4 catalysts are shown in Table 3. The values obtained for the spent catalysts were considerably affected by the amount of material absorbed on the catalyst, as it was found by TGA analysis. Thus they were normalized to the amount of adsorbed organic carbon and water. The metal content in the spent catalysts was calculated in the following way:

$$C_{Pt,spent\ norm} = 100 * \frac{1-a-m}{1-d-k-n}; \quad (7)$$

where *a* and *d* is the Pt content determined by ICP in the fresh and the spent catalyst, *m* and *n* are the water content in the fresh and the spent catalyst, and *k* is the percentage of adsorbed species in the spent catalyst.

Both catalysts did not show any significant metal losses.

Table 3. ICP analysis of fresh and spent Pt/AC catalysts.

Catalyst	*Condition*	*ICP Pt content, [wt %]*

Pt/AC-1	**fresh**	**2.4**
	spent, 2h / **normed**	2.16 / **2.36**
Pt/AC-4	**fresh**	**2.72**
	spent 3x2 h, cage / **normed**	1.92 / **2.49**

3.2. Preparation of technical sorbitol-mannitol mixture

Sugars obtained from biomass, e.g. sucrose from sugarcane, are easily accessible and comparably cheap. According to the literature, APR of sugars is leading to fast catalyst deactivation due to high coke formation and generation of multiple condensation products. Addition of a preliminary hydrogenation step can substantially increase the overall hydrogen production and catalysts stability. APR of a polyol appears to be more beneficial compared to the direct APR of the starting sugar. Hydrogenation of sugars is a well-known process, which leads to formation of a mixture of polyols.

Hydrogenation of sucrose is schematically represented in Figure 3. The sucrose conversion, yields of the main and by-products and balances, are given in Table 4. An overall conversion of sucrose up to 98% was obtained, resulting in a polyol yield of 92%. Sorbitol dominates among the products, mannitol is the second major product. Some minor side products were observed, the two most abundant ones being 1,2-propanediol and ethanol. Formation of 1,2-propanediol and glycerol can be explained by the retro-aldol condensation. Traces of glucose and sucrose were found as well.

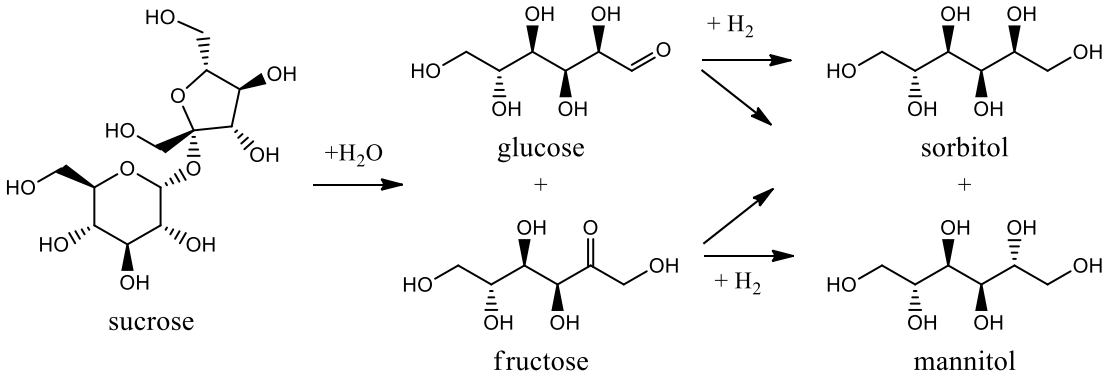

Figure 3. Scheme of sucrose hydrogenation (adapted from [62]).

Table 4. Results of the production of technical sorbitol/mannitol mixture from sucrose.

Parameter	Value
	Initial feed
concentration of sucrose [wt %]	51.3
	Product
conversion of sucrose [%]	98.0
concentration of polyol [wt %]	49.3
yield of polyol [%]	92*
concentration of by-products [wt %]	3
	Polyol distribution
yield of sorbitol [wt %]	62.4
yield of mannitol [wt %]	37.6
	Yields of identified liquid by-products
yield of 1,2-propanediol [%]	0.4
yield of ethanol [%]	0.2
yield of glycerol [%]	0.1
	Yields of identified gaseous by-products
yield of CH_4 [%]	1.0
yield of CO [%]	0.05
	Overall balances
mass balance [%]	97
carbon balance [%]	88
hydrogen balance [%]	103
oxygen balance [%]	99

* A white solid was crystallized in the reactor tubing, which is probably mannitol. Therefore, the total yield of polyols is expected to be higher.

3.3. Aqueous-phase reforming of technical sorbitol-mannitol mixture

Catalytic reforming of polyols proceeds through the formation of various liquid-phase intermediates, giving gas-phase products, such as hydrogen, CO, CO_2, and alkanes (Figure 4).

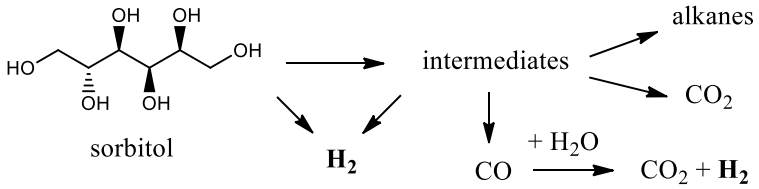

Figure 4. A simplified scheme of products formed in the APR of sorbitol.

The commercial sorbitol and the technical polyol feed mixture were compared in terms of gas production, conversion of polyols and selectivity to hydrogen, CO_2 and alkanes. The comparison is given below for the results obtained in the continuous reactor.

The technical and the commercial feed were showing a similar conversion (Figure 5a). It should be noted that although the same catalyst sample was utilized for both experiments, the activity was restored during the regeneration procedure, previously implemented successfully [63]. Flushing with water removes water-soluble components, while acetone dissolves hydrophobic compounds, and the metal is reduced to the zero-valent state. Coke formation is not pronounced in the case of APR of pure sorbitol, as it was shown in [53,54].

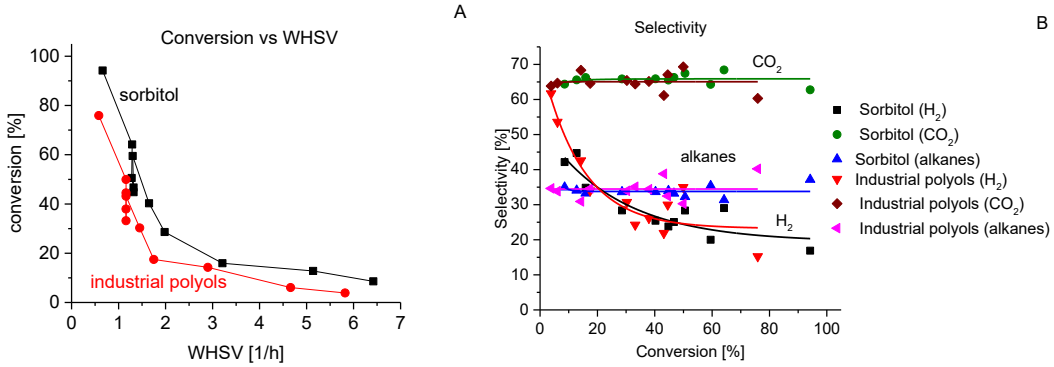

Figure 5. APR of sorbitol or technical polyols over Pt/AC-JM. A: conversion of sorbitol or technical polyols versus WHSV. B: selectivity to hydrogen, CO_2 and total selectivity to alkanes versus conversion of sorbitol or sorbitol/mannitol. The following conditions were applied: T = 498K, P = 29.7 bar, mass of catalyst 0.5 g.

Both sorbitol and technical polyols displayed a similar selectivity to the main final products, such as alkanes, CO_2 and hydrogen (Figure 5b). As reported earlier by our group [64], the chirality of the initial polyol has a noticeable influence on the distribution of the liquid-phase products, while selectivity to the final products is unaffected. Similar results were obtained for the individual alkanes ranging from C_1 to C_6 (Figure 6). The catalyst was mostly selective to n-butane and propane, with slightly lower values obtained for methane and ethane. The selectivity to pentane was significantly lower compared to other linear alkanes. The product of the full hydrogenation of the initial polyol, n-hexane, was formed in substantial amounts. Traces of neo-pentane were found among other alkanes. The overall alkane distribution is similar in the case of both feeds.

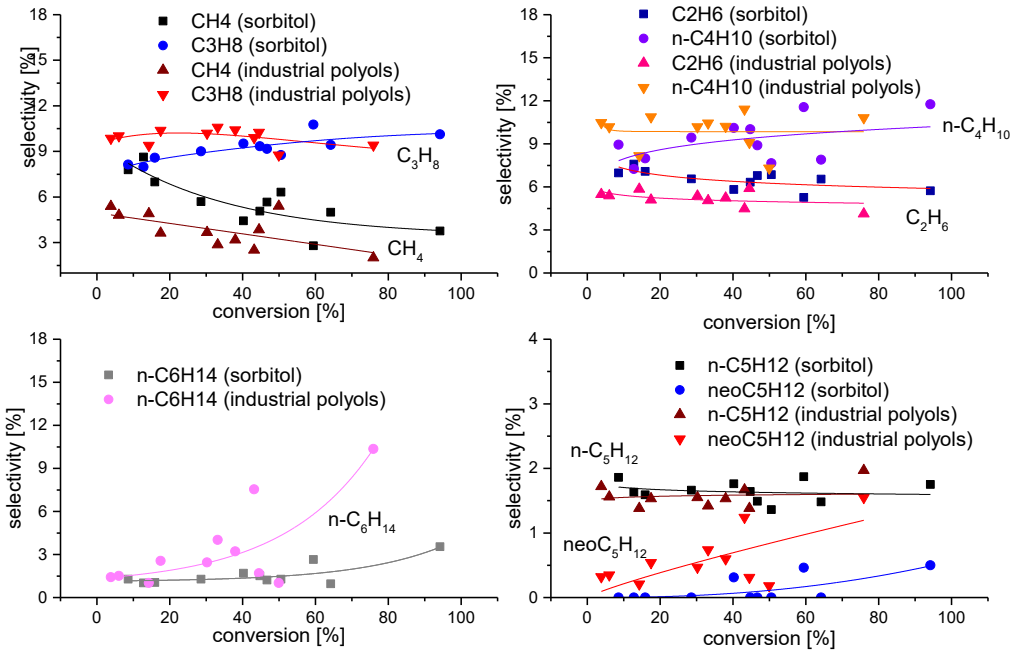

Figure 6. Selectivity to individual alkanes C_1-C_6 in the APR of sorbitol or the technical polyols over Pt/AC-JM versus conversion. The following conditions were applied: T = 498K, P = 29.7 bar, mass of catalyst 0.5 g.

The catalyst activity is decreasing along with time-on-stream (Figure 7), being slightly lower in the case of the technical feed. Similarly, a lower overall gas production was obtained with technical polyols mixture (Figures 8 and 9), however, similar patterns are obtained for both feeds, indicating a comparable catalyst deactivation mechanism.

The decrease in conversion is more pronounced after the periods, when a higher feeding flow rates were applied, being practically restored to the original values after long periods with a low flow rate. Catalytic activity obtained in this study correlates well with the data of sorbitol APR obtained over 1% Pt/Al_2O_3 in [64]. A similar enhancement effect was observed for the gas production from sorbitol after long periods of low flow rates. These phenomena were not reported previously, and require additional experimental efforts.

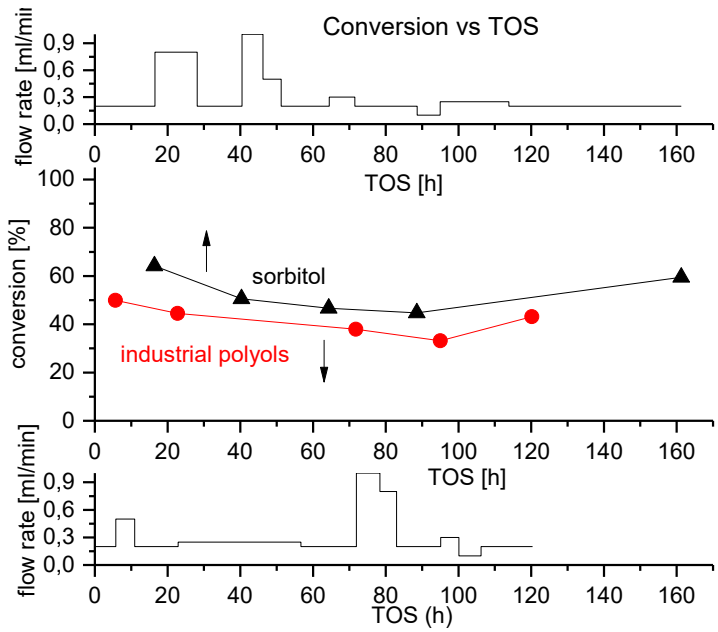

Figure 7. Conversion of sorbitol and technical polyols in APR over Pt/AC-JM versus TOS. The flow rates applied during the experiment are shown above and below concentration dependences for sorbitol and the technical mixture respectively. The following conditions were applied: T = 498K, P = 29.7 bar, mass of catalyst 0.5 g.

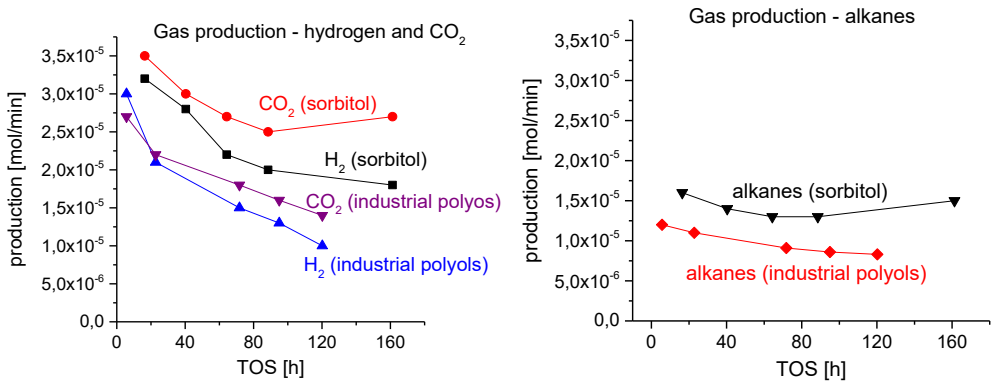

Figure 8. Hydrogen, CO_2 and total alkanes production from sorbitol or technical polyols in APR over Pt/AC-JM versus TOS. The following conditions were used: T = 498K, P = 29.7 bar, mass of catalyst 0.5 g.

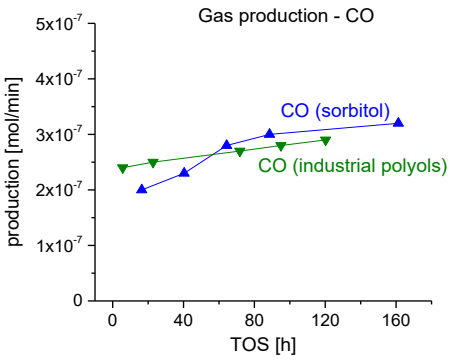

Figure 9. CO production from sorbitol or technical polyols in APR over Pt/AC-JM versus TOS. The following conditions were used: T = 498K, P = 29.7 bar, mass of catalyst 0.5 g.

A comparison of sorbitol APR in a nitrogen atmosphere to glucose and sorbitol hydrodeoxygenation is described in literature [14]. Here, a similar selectivity to hydrogen and alkanes was obtained.

Comparison of the data obtained in this research with data from the literature is rather difficult and limited. The results obtained here can only be directly compared with literature data, if the following requirements are met, use of: the same feed [8,9], substrate concentration [37], temperature [39], reactor type [65–67], active metal [68], and type of support [9,69,70] .

The catalysts activity found in this study correlates well with the data of sorbitol APR obtained over a 1% Pt/Al_2O_3 in [64]. A similar initial feed concentration of 3.6 wt % was applied, while the metal loading was higher in the case of 2.5 wt % Pt/AC-JM. Similar conversion levels of ca. 15 and 95% were obtained at comparable WSHV's. The selectivity to hydrogen is much lower over the Pt/AC-JM compared to Pt/Al_2O_3, which is accompanied by an opposite trend of selectivity to alkanes. According to [71], platinum catalysts supported on activated carbon and on alumina exhibited a similar selectivity to hydrogen, while Pt/Al_2O_3 was slightly less selective to alkanes. However,

it is known that the acidity of the supports can significantly influence alkane selectivity [43], making direct comparison difficult.

A part of the liquid-phase intermediates obtained in the APR of sorbitol and the technical polyols were identified. The amount of identified carbon in the intermediates varied from 21 to 52% depending on the conversion. The yields of identified substances are presented in Figure 10. The intermediates are subdivided into the following groups: sugars and sugar alcohols, alcohols C_2-C_3, alcohols C_4-C_6, aldehydes/ketones, acids, and heterocyclic compounds. It should be noted that a small amount of glucose, arabitol and glycerol was already present in technical polyol feed. The corresponding values were subtracted from their concentrations in the final solution. Poor separation of arabitol, xylitol, and arabinose from sorbitol and mannitol in the HPLC analysis led to rather high errors in the concentration of those substances, especially at low conversion levels.

Certain sugar alcohols were found among other intermediates, namely xylitol, arabitol and erythritol (Figure 10 a). The general trend is that yields of shorter sugar alcohols are increasing along with conversion of the initial polyol. Xylitol and arabitol can be treated as primary intermediates.

Yields of primary intermediates formed through dehydrogenation of the initial feed should be decreasing along with the conversion. Yields of mannose and glucose are following this trend except for glucose in the technical polyols, which is altered by the presence of glucose in the initial solution (Figure 10b). Formation of mannose from pure sorbitol can be explained by diastereomerisation and subsequent dehydrogenation [62].

Linear alcohols C_3-C_6, including diols and triols, were obtained in similar amounts regardless the initial feed (Figure 10c and d). Linear and branched carbonyls, namely

3-hydroxy-2-butanone and isobutyraldehyde (Figure 10e), along with fumaric and acetic acids (Figure 10f) are also detected in similar amounts. It is rather interesting that isobutanol or branched alkanes were not found. The yield of glycerol was similar in both cases.

The yields of 5-hydroxymethyl-2-furaldehyde and 2-acetylfuran were approximately a twofold higher in the case of the technical polyols feed while 2,5-dimethylfuran was detected in similar amounts in the both cases (Figure 10g).

Comparison of the liquid-phase intermediates did not show any major differences between the APR of commercial sorbitol and technical polyols.

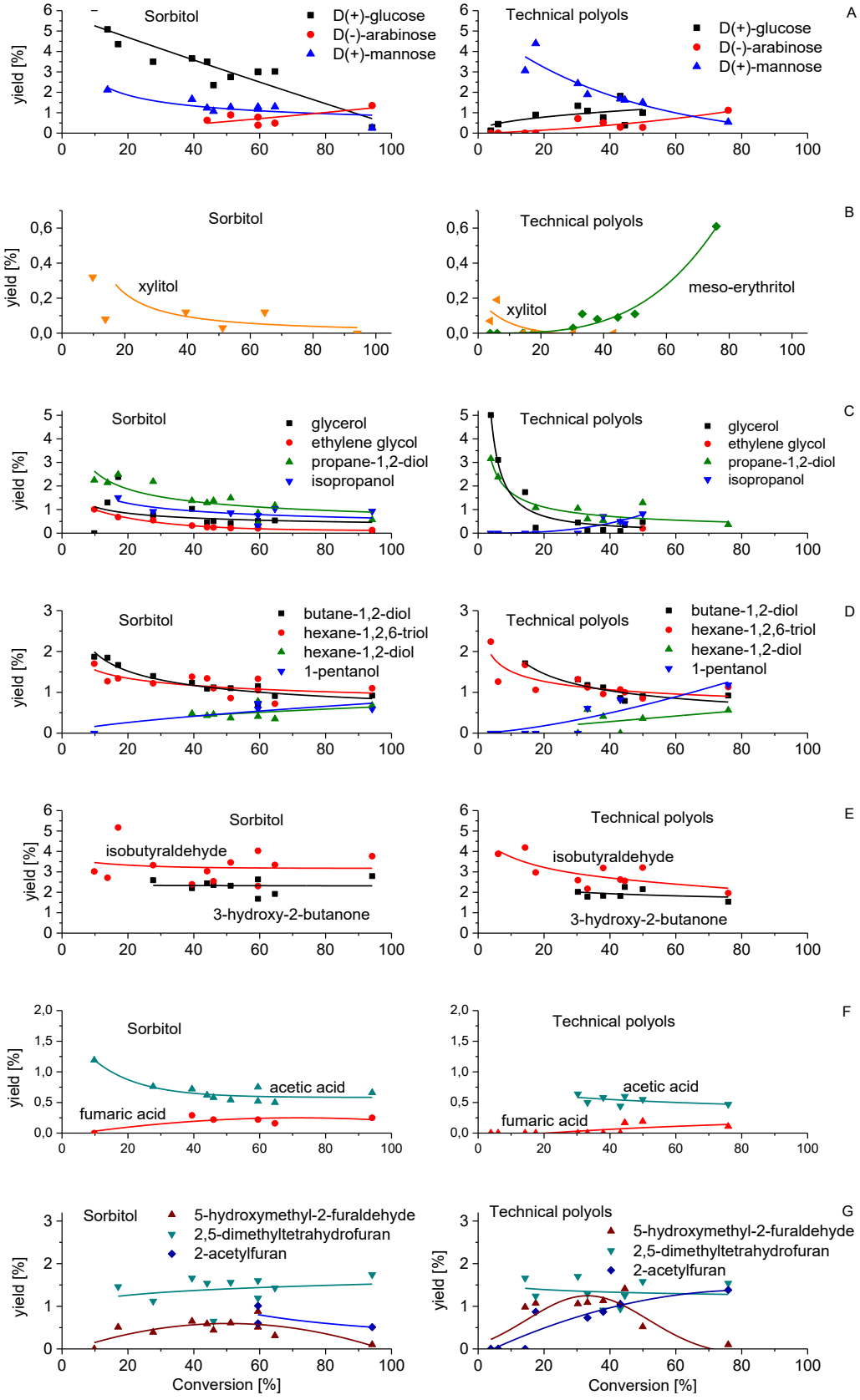

Figure 10. Yields of the liquid-phase intermediates as a function of polyols conversion. Substances obtained in the sorbitol APR over Pt/AC-JM are shown on the left side, in

the APR of technical polyols – on the right side. All intermediates are separated to the following groups: a – sugar alcohols, b – sugars, c – acids, d – alcohols C_2-C_3, e – alcohols C_4-C_6, f – aldehydes/ketones, g – heterocyclic compounds. The following conditions were used: T = 498K, P = 29.7 bar, mass of catalyst 0.5 g.

A comparison of data obtained in the sorbitol APR over Pt/AC-JM and Pt/Al_2O_3 [64] at similar conversion levels revealed a significant difference in the liquid-phase composition (Table 5). Only 30% of carbon contained in the liquid-phase intermediates was identified in the case of the carbon-supported catalyst, which is twofold lower compared to Pt/Al_2O_3. Higher yields of sugar alcohols, acids and other alcohols were observed with the Pt/Al_2O_3, while formation of sugars and substituted furans was more pronounced for Pt/AC-JM. The overall degree of carbon conversion to the gas phase was higher over alumina-supported catalyst.

Table 5. Yields of the liquid-phase intermediates obtained during sorbitol APR over Pt/Al_2O_3 [64] and Pt/AC-JM at similar conversion: 62 and 65 % correspondingly.

	Pt/Al_2O_3	*Pt/AC-JM*
Substance	*yield [%]*	*yield [%]*
sugars		
D(-)-arabinose		0.49
D(+)-glucose	0.36	3.04
mannose		1.30
sugar alcohols		
D(+)-arabitol	0.40	0.08
meso-erythritol	2.09	
xylitol	2.87	0.12
acids		
acetic acid	0.90	0.50
caproic acid	0.14	
fumaric acid	1.52	0.16
lactic acid	0.16	traces
pyruvic acid	0.13	
tartaric acid	0.06	
alcohols		
1-pentanol	0.17	traces
1-propanol	2.86	
2-pentanol	0.05	
butane-1,2-diol	1.40	0.91
ethanol	3.32	
ethylene glycol		traces
glycerol	2.89	0.55
hexane-1,2-diol	0.29	0.35
hexane-1,2,6-triol		0.73
hexane-2,5-diol	0.62	
isopropanol		1.04
methanol	2.85	0.89
propane-1,2-diol	2.23	1.17
aldehydes/ketones		
3-hydroxy-2-butanone	3.48	1.93
acetone	0.41	
isobutyraldehyde		3.36
furans		
2-acetylfuran	0.06	
2,5-dimethyltetrahydrofuran	0.12	1.44
5-hydroxymethyl-2-furaldehyde	0.24	0.31
tetrahydrofurfuryl alcohol	0.48	
SUM	30	18.4
Identification degree [%]	62	30
Total carbon content in the liquid-phase intermediates [%]	30.3	40

Additionally, APR of a concentrated technical polyols mixture (29 wt %) was performed over the Pt/AC-JM catalyst. The overall polyol conversion determined by HPLC, the gas production and selectivity to the main gas products are presented in Figure 11.

The initial conversion level (9%) of the concentrated feed was, as expected, lower compared to the diluted feed. The conversion dropped to zero after 70 hours of time-on-stream (Figure 11 a). Some gas production was observed even at apparently zero conversion (Figure 11 b), mainly due to low accuracy of HPLC analysis. Selectivity to hydrogen, CO, CO_2 and alkanes was practically not altered by catalyst deactivation (Figure 11 c), while the distribution of alkanes changed significantly with n-hexane being predominantly formed (Figure 11 d).

Initial selectivity to hydrogen was noticeably lower in the case of the concentrated technical feed (10%) compared to the diluted one (50%), while selectivity to alkanes showed an opposite trend, being 40 and 35% for the concentrated and the diluted feed correspondingly. Selectivity to CO_2 was equal in the both cases.

Higher feed concentration led to an increase in the overall reaction rate and, subsequently, gas production in the case of APR of glycerol in a wide range of concentrations (10-30%) [72]. These results are not directly in line with APR of diluted sorbitol solutions over Pt/Al_2O_3, showing that hydrogen production was not affected by an increase in sorbitol concentration from 1 to 5% [54].

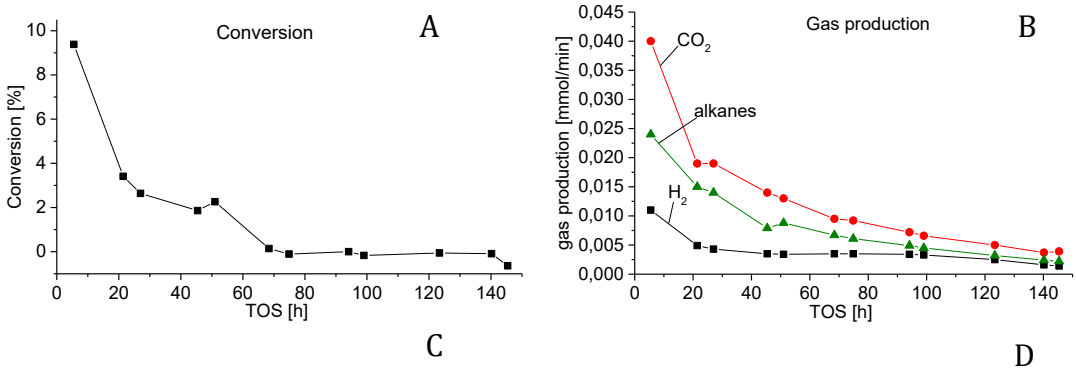

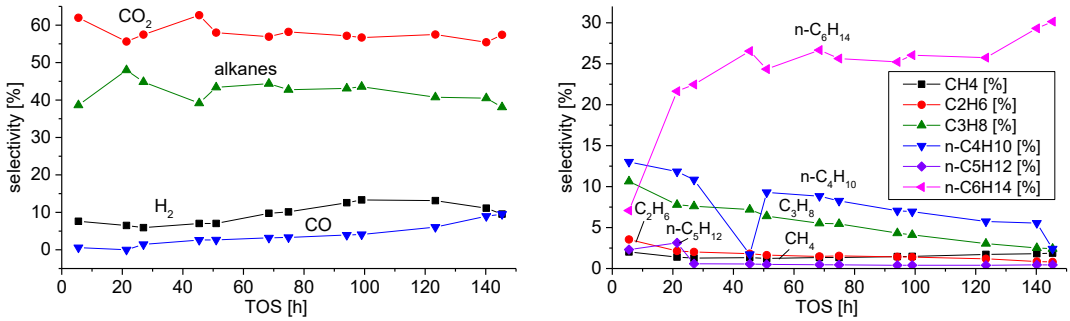

Figure 11. Aqueous-phase reforming of the 29 wt % solution of the technical polyols mixture: a – conversion, b – gas production, c – selectivity to CO_2, H_2, CO, alkanes, d – selectivity to individual alkanes. The following conditions were used: T = 498K, P = 29.7 bar, mass of catalyst 0.5 g.

Slightly lower conversion levels and gas productivity were obtained in the APR of the technical polyols mixture compared to commercial sorbitol over a Pt/C catalyst. Both feeds were equally selective to gas products and showed practically equal yields of the liquid products. The minor amounts of impurities in the technical polyol mixture were not giving any notable complications in APR. The technical feed is not showing any significant differences from the model polyol, indicating a large potential of its application as feed in APR for hydrogen production.

3.4. Batch reactor

The results of the technical feed conversion in the batch mode are shown in Figure 12. The amount of gas products produced in the experiments was normalized to the initial concentration of the feed. The carbon conversion from the liquid to the gas phase was significantly higher over Pt catalysts compared to a blank non-catalytic reaction (Figure 12a). However, the conversion of sorbitol/mannitol reached 10% in the blank experiment, which is rather significant in comparison with the value achieved over Pt catalysts (26-28%). Negligible quantities of identified gas products, such as hydrogen,

CO_2 and methane, were obtained in the blank experiment (Figure 12d, g). The amount of other alkanes was insignificant in all tests. CO_2 was the main gas-phase product (Figure 12d) in the catalyzed experiments, the observed amount of hydrogen and methane was considerably lower (Figure 12g).

Three consecutive reuse cycles of the Pt/AC-4 catalyst are given in Figure 12b. The catalyst was losing activity with each run in terms of carbon conversion, however, the sorbitol conversion was increasing. The hydrogen production was halved after the first run in the reuse experiment (Figure 12h), while a stable production of methane and CO_2 was observed (Figure 12e, h). This could probably be explained by the changes in the Pt particle size and coke formation.

Carbon conversion (Figure 12c) is increasing with time along with methane (Figure 12i) and CO_2 (Figure 12f) production over the Pt/AC-4, while the observed amount of hydrogen is decreasing after a sharp initial increase (Figure 12i). In several studies found in literature, it was already concluded that batch reactors are not preferred for hydrogen production due to hydrogen involvement in secondary reactions [65–67]. The results of the current study are in line with the literature.

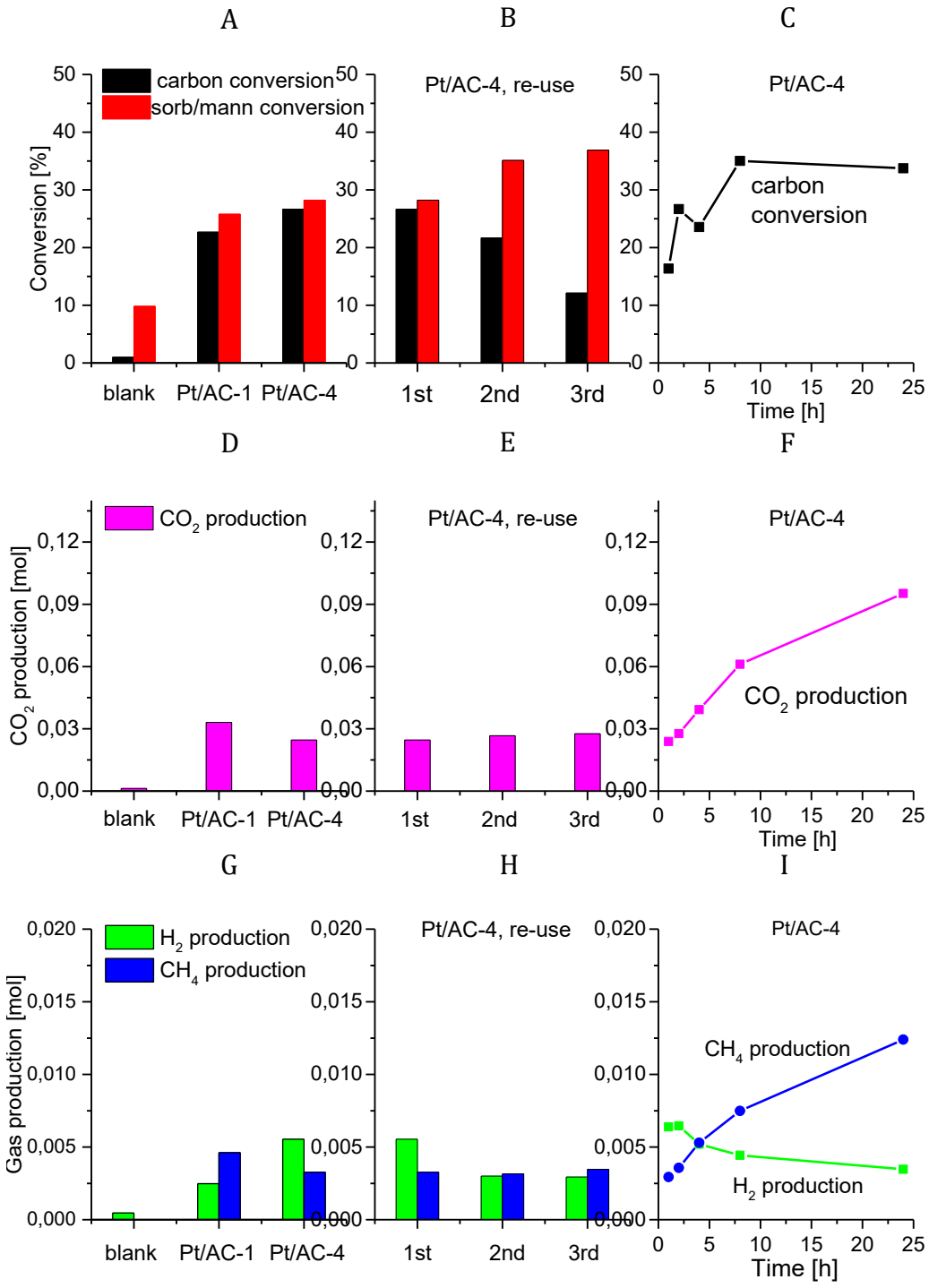

Figure 12. APR of the technical sorbitol/mannitol mixture in the batch reactor at 498 K. Left side: blank test and APR over Pt/AC-1 and Pt/AC-4. Middle: stability of Pt/AC-4. Right side: performance of Pt/AC-4 during 24 hours. Upper row: carbon and sorbitol/mannitol conversion. Middle row: CO_2 production. Lower row: H_2 and CH_4 production. Experiments were performed in 380 mL autoclave. 150 mL of feed (15.3 mol/L) was used in blank test and Pt/AC-1. 200 mL of feed (4.0-5.6 mol/L) was used in experiments over Pt/AC-4. Gas production was normalized to initial concentration of 15.3 mol/L.

The total amount of identified carbon contained in the liquid-phase intermediates was 11-18%. Higher yields of glycerol (1.2%), acetic acid (4%), and 1,2-propanediol (4.9%) were obtained in the batch test over Pt/AC-4 catalyst compared to the tests performed in the continuous reactor (0.5, 0.6, and 1.0% correspondingly) at similar conversion levels. In addition, ethylene glycol (1.3%), acetone (1.1%), and xylitol (0.8%) were identified in the liquid-phase products obtained in the batch reactor. A higher alcohol content could be assigned to hydrogenation reactions, more pronounced in the batch mode compared to the continuous one. The overall fraction of carbon transformed to the gas phase was approximately a twofold lower in batch mode (3.8%) compared to the continuous mode (6.5%) at a comparable conversion level of ca. 29%.

The carbon distribution along with the total carbon balance is shown in Figure 13. The amount of carbon transformed to the gas phase was estimated by GC, while the aqueous products were analysed by CHN. The rest was supplemented by the theoretical amount of carbon, which could be adsorbed by the catalyst. The majority of carbon was retained in the liquid phase. Less than 15% of the starting carbon was converted to the gas-phase products after 24 h of reaction. The total carbon balance reached 99% in the blank test and was close to 80-90% in other experiments, with the exception of the 8 h experiment with Pt/AC-4.

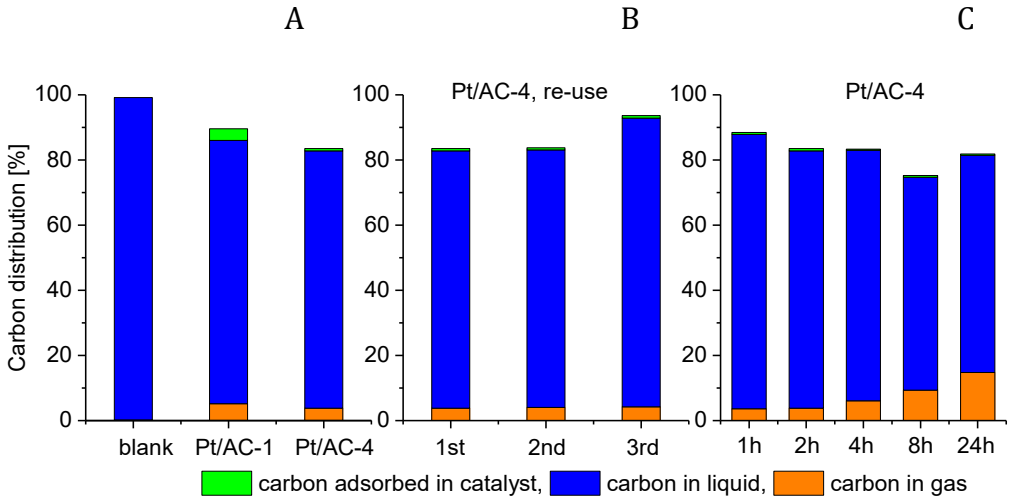

Figure 13. Carbon distribution and total carbon balance in the APR of the technical sorbitol/mannitol mixture in the batch reactor at 498 K. A: blank test and APR over Pt/AC-1 and -4. B: stability of Pt/AC-4. C: performance of Pt/AC-4 during 24 hours. Experiments were performed in 380 mL autoclave. 150 mL of feed (5 mol C/L) was used in blank test and Pt/AC-1. 200 mL of feed (1.2-1.8 mol C/L) was used in experiments over Pt/AC-4. Gas production was normalized to initial concentration of 5 mol C/L.

The amount of carbon adsorbed by the Pt/AC-1 catalyst was 0.03 mol C according to TGA analysis. A similar value of 0.03 mol C (C_{cat}, mol) was obtained by a rough estimation based on the amount of absorbed water by the carbon support (x_{water}, g water/g cat), the carbon content in the final solution (CC_{fin}, wt %), and the catalyst amount (m_{cat}, g):

$$C_{cat} = CC_{fin} \cdot \frac{x_{water} \cdot m_{cat}}{100 * 12} \quad (8)$$

This value correlates well also with the experimental data obtained for adsorption of ethanol by activated carbon from aqueous solutions [73].

The amount of carbon adsorbed/absorbed by the catalyst is negligibly low and is insignificant for the carbon balance calculated for all experiments except for the experiment over the Pt/AC-1.

Application of the Pt/AC-4 catalyst with the particle size 1-2 mm could potentially cause internal mass-transfer limitations. The Weisz-Prater criterion value is equal to

1.25, which confirms the presence of internal mass-transfer limitations. For a first-order reaction not limited by mass-transfer this value should be below 0.6. The details of this calculation can be found in the supporting information. The real value of the Weisz-Prater criterion is at least one order of magnitude larger, since it was based on the observed reaction rate at 2 h of reaction. Thus, certain mass-transfer limitations are taking place in the experiment performed batch-wise with the Pt/AC-4 catalyst.

3.5. Hydrogen production

The hydrogen balance can be presented in the following way. One mole of hydrogen is utilized in order to obtain one mole of sorbitol or galactitol from 0.5 moles of the disaccharide sucrose. A similar ratio with the coefficient equal to 1 is valid for monosaccharides and corresponding polyols. According to the theoretical representation of APR, it is thus possible to produce 13 moles of hydrogen from 1 mole of sorbitol. The overall hydrogen balance is positive when more than one mole of hydrogen is produced from one mole of sorbitol in APR, however, a higher ratio is beneficial:

$0.5\ C_{12}H_{22}O_{11} + 0.5\ H_2O + H_2 \rightarrow C_6H_{14}O_6$

$C_6H_{14}O_6 + 6\ H_2O \rightarrow 6\ CO_2 + 13\ H_2$

The experimental data generated in the current work as well as found in the literature for continuous reactors over various catalysts are presented in Figure 14. More details can be found in Table 6. The ratio of generated H_2 to converted sorbitol (H/S) is given as a function of sorbitol conversion. The H/S value for sorbitol could theoretically range from 0 to 13 according to the equations presented above.

Both the commercial sorbitol and technical polyol mixture, processed by applying the Pt/AC-JM catalyst showed very low values of H/S being close to 1 with a slight increase

at low conversion levels. Thus, the amount of produced hydrogen production in the current study barely covers the need for sucrose hydrogenation, making the overall process completely inefficient.

However, data obtained over Pt/Al_2O_3 (denoted as Duarte 2016, Godina 2015, Kirilin 2010, and Kirilin 2012 in Figure 14) appeared to be more promising in terms of hydrogen production with the maximum H/S value equal to 9. A certain discrepancy of results obtained in different set-ups has to be studied further. A decreasing dependence was obtained by Duarte et al. [54], a linear one by Godina et al. [64], and a maximum by Kirilin et al. [63]. Similar catalysts and conditions were applied except for splitting with an inert gas, which was performed at a lower ratio of the inert to liquid flows in [54] compared to other studies (see Table 6). It should be noted that the inert splitting was 20-30 mL/min (STP) in all studies.

Purging of an inert carrier gas is beneficial for hydrogen production, as shown in [66] for APR in a wash-coated reactor over Pt/AlOOH catalyst (Neira 2014 H_2 strip in Figure 14). Application of a membrane reactor [74] allowed effective separation of gas phase from liquid medium during APR over Pt/C, which significantly improved hydrogen production (Neira 2014 m in Figure 14).

Similar low values of H/S were obtained over Pt/AC-JM and Pt/C (denoted as Neira 2014 m in Figure 14) catalysts, while the same Pt/C performed better at higher conversion levels (Neira 2014 in Figure 14) giving H/S equal to 2.5-3.5. Absence of details about the experimental studies does not allow, however, an adequate explanation of these observations.

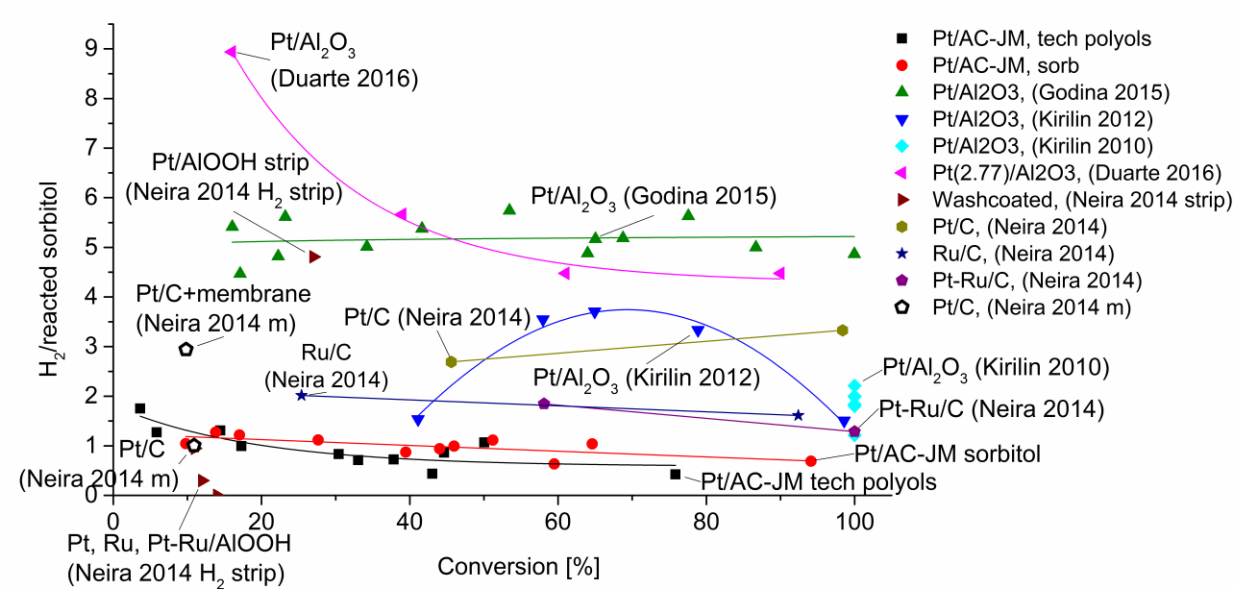

Figure 14. Amount of produced hydrogen from reacted sorbitol as a function of polyol conversion. Data were collected from the following publications: Kirilin 2010 [75], Kirilin 2012 [63], Duarte 2016 [54], Neira 2014 strip [66], Neira 2014 [76], Neira 2014 m [74], Godina 2015 [64]. *Pt/C+membrane* denotes application of a membrane reactor for direct hydrogen separation during APR. *Pt/AlOOH strip* stays for stripping with an inert gas.

Table 6. Experimental conditions found from the literature for comparison of hydrogen production per mole of converted sorbitol.

Catalyst	*Publication*	*Inert splitting [m^3 gas/m^3 liquid [1]]*	*Flow rates of liquid phase [mL/min, STP]*	*Feature related to hydrogen production*
Pt/AC-JM	current study	6.4-0.64	0.1-1	Role of impurities
Pt/Al_2O_3	Kirilin 2010 [75]	10-2	0.1-0.35	
Pt/Al_2O_3	Kirilin 2012 [63]	10-2.9	0.2-0.5	
Pt/Al_2O_3	Duarte 2016 [54]	0.11-0.03	0.1-0.4	Role of Pt dispersion
Pt/AlOOH Ru/AlOOH Pt-Ru/AlOOH	Neira 2014 strip [66]	2 for Pt/AlOOH strip, 0 for others		Role of inert splitting
Pt/C Ru/C Pt/C+Ru/C	Neira 2014 [76]	2		Role of the catalyst
Pt/C	Neira 2014 m [74]	9	0.3	Role of gas-phase removal
Pt/Al_2O_3	Godina 2015 [64]	10-1	0.1-1	

[1] Volume ratio at reaction conditions

It could be concluded that carbon-supported Pt catalysts are most probably not selective enough to hydrogen for utilization in polyol APR, despite the combination of their strong mechanical properties (e.g. Sibunit or polymer-based activated carbons) and high hydrothermal stability. However, removal of the gas phase during the reaction, decreasing of hydrogen partial pressure via application of a carrier gas, and operation under low conversion levels could help to maximize the hydrogen yield.

Another important aspect is feasibility of the process. Hydrogen production from polyol via APR is becoming competitive with methane steam reforming if the polyol price is less than 0.3$/kg per kg according to the calculations provided in [77]. The current sucrose price is 0.28 $/kg according to [78]. The target polyol price of 0.3$/kg is clearly not achievable via sucrose hydrogenation, nevertheless, the APR process has a high potential for the production of renewable hydrogen in the near future in case of economically competitive feedstock.

4. Conclusions

An aqueous solution of sorbitol and a mixture of sorbitol/mannitol (technical polyols), produced by the hydrogenation of a sucrose solution, were used as the feed in APR to produce hydrogen in batch and continuous reactors over Pt/C catalysts. A detailed comparison was made between the feed conversion, selectivity to the main products and the yields of liquid-phase intermediates. To the best of our knowledge this was not earlier reported in literature. The hydrogen selectivity obtained at 14% conversion level was 42-44% for both the feedstocks. The 2.5 wt % Pt/C catalyst was equally selective to the main gas-phase products in APR for both feedstocks, while minor differences were found in the yields to some liquid-phase intermediates, accompanied by a slightly different distribution of alkanes. Application of the technical feed also resulted in slightly lower activity.

Batch-wise processing appeared to be considerably less effective for hydrogen production compared to the continuous mode. The main reason for this is the fast consumption of produced hydrogen in various hydrogenation reactions.

A small amount of impurities in the initial feed was not an obstacle for the APR of the technical mixture of polyols, as was confirmed by comparing data obtained with the technical feed and commercial sorbitol in the continuous reactor. The technical feed was not showing significant differences from the model polyol, indicating a strong potential of its application as a feed in APR to produce hydrogen.

However, the process described in this work cannot be utilized directly for hydrogen production, since the amount of produced H_2 per one mole of converted sorbitol is barely enough to perform sucrose hydrogenation. Pt/Al_2O_3 or other metal- or mixed oxides-supported catalysts are more promising, while application of carbon-supported catalysts will probably require additional efforts, such as decreasing of hydrogen partial

pressure via removal of the gas phase during the reaction, application of a carrier gas, or operating under low conversion levels.

Acknowledgements

This work was supported by the European Union's Seventh Framework Programme for research, technological development and demonstration under Grant Agreement No. 310490 (SusFuelCat Project www.susfuelcat.eu).

The authors are grateful to Dr. I. Simakova from Boreskov Institute of Catalysis for TEM analysis, and colleagues from Laboratory of Wood and Paper Chemistry, Åbo Akademi University for technical support.

References

[1] Lynd LR, Wyman CE, Gerngross TU. Biocommodity engineering. Biotechnol Prog 1999:777–793.

[2] Zabed H, Sahu JN, Boyce AN, Faruq G. Fuel ethanol production from lignocellulosic biomass: An overview on feedstocks and technological approaches. Renew Sustain Energy Rev 2016;66:751–774.

[3] Wawrzetz A. Aqueous phase reforming of glycerol over supported catalysts, Ph.D thesis. Technischen Universität München, 2008.

[4] Tanksale A, Beltramini JN, Lu GM. A review of catalytic hydrogen production processes from biomass. Renew Sustain Energy Rev 2010;14:166–182.

[5] Vilcocq L, Cabiac A, Especel C, Guillon E, Duprez D. Transformation of sorbitol to biofuels by heterogeneous catalysis: chemical and industrial considerations. Oil Gas Sci Technol 2013;68:841–860.

[6] Davda RR, Shabaker JW, Huber GW, Cortright RD, Dumesic JA. A review of catalytic issues and process conditions for renewable hydrogen and alkanes by aqueous-phase reforming of oxygenated hydrocarbons over supported metal catalysts. Appl Catal B Environ 2005;56:171–186.

[7] Wei Y, Lei H, Liu Y, Wang L, Zhu L, Zhang X, Yadavalli G, Ahring B, Chen S. Renewable hydrogen produced from different renewable feedstock by aqueous-phase reforming process. J Sustain Bioenergy Syst 2014;4:113–127.

[8] Cortright RD, Davda RR, Dumesic JA. Hydrogen from catalytic reforming of biomass-derived hydrocarbons in liquid water. Nature 2002;418:964–967.

[9] Kim H-D, Park HJ, Kim T-W, Jeong K-E, Chae H-J, Jeong S-Y, et al. The effect of support and reaction conditions on aqueous phase reforming of polyol over supported Pt–Re bimetallic catalysts. Catal Today 2012;185:73–80.

[10] Tanksale A, Wong Y, Beltramini JN, Lu GQ. Hydrogen generation from liquid

phase catalytic reforming of sugar solutions using metal-supported catalysts. Int J Hydrogen Energy 2007;32:717–724.

[11] Esteve-Adell I, Crapart B, Primo A, Serp P, Garcia H. Aqueous phase reforming of glycerol using doped graphenes as metal-free catalysts. Green Chem 2017;19:3061–3068.

[12] Meryemoglu B, Irmak S, Hasanoglu A, Erbatur O, Kaya B. Influence of particle size of support on reforming activity and selectivity of activated carbon supported platinum catalyst in APR. Fuel 2014;134:354–357.

[13] Wen G, Xu Y, Xu Z, Tian Z. Direct conversion of cellulose into hydrogen by aqueous-phase reforming process. Catal Commun 2010;11:522–526.

[14] Davda RR, Dumesic JA, Drive E. Renewable hydrogen by aqueous-phase reforming of glucose. Chem Commun 2004:2003–2004.

[15] Valenzuela MB, Jones CW, Agrawal PK. Batch aqueous-phase reforming of woody biomass. Energy & Fuels 2006;42:1744–1752.

[16] Wen G, Xu Y, Xu Z, Tian Z. Characterization and catalytic properties of the Ni/Al2O3 catalysts for aqueous-phase reforming of glucose. Catal Letters 2008;129:250–257.

[17] Kaya B, Irmak S, Hasanoğlu A, Erbatur O. Developing Pt based bimetallic and trimetallic carbon supported catalysts for aqueous-phase reforming of biomass-derived compounds. Int J Hydrogen Energy 2015;40:3849–3858.

[18] Remon J, Ruiz J, Oliva M, Garcia L, Arauzo J. Cheese whey valorisation: Production of valuable gaseous and liquid chemicals from lactose by aqueous phase reforming. Energy Convers Manag 2016;124:453–469.

[19] Remon J, Garcia L, Arauzo J. Cheese whey management by catalytic steam reforming and aqueous phase reforming. Fuel Process Technol 2016;154:66–81.

[20] Lai Q, Skoglund MD, Zhang C, Morris AR, Holles JH. Use of hydrogen chemisorption and ethylene hydrogenation as predictors for aqueous phase reforming of lactose over Ni@Pt and Co@Pt bimetallic overlayer catalysts. Energy & Fuels 2016;30:8587–8596.

[21] Kaya B, Irmak S, Hasanoglu A, Erbatur O. Evaluation of various carbon materials supported Pt catalyts for aqueous-phase reforming of lignocellulosic biomass hydrolysate. Int J Hydrogen Energy 2014;39:10135–10140.

[22] Meryemoglu B, Irmak S, Hasanoglu A. Production of activated carbon materials from kenaf biomass to be used as catalyst support in aqueous-phase reforming process. Fuel Process Technol 2016;151:59–63.

[23] Irmak S, Meryemoglu B, Hasanoglu A, Erbatur O. Does reduced or non-reduced biomass feed produce more gas in aqueous-phase reforming process? Fuel 2015;139:160–163.

[24] Meryemoğlu B, Hasanoğlu A, Kaya B, Irmak S, Erbatur O. Hydrogen production from aqueous-phase reforming of sorghum biomass: An application of the response surface methodology. Renew Energy 2014;62:535–541.

[25] Chang AC-C, Louh RF, Wong D, Tseng J, Lee YS. Hydrogen production by aqueous-phase biomass reforming over carbon textile supported Pt–Ru bimetallic catalysts. Int J Hydrogen Energy 2011;36:8794–8799.

[26] You SJ, Baek IG, Kim YT, Jeong K-E, Chae H-J, Kim T-W, Kim C-U, Jeong S-Y, Kim TJ, Chung Y-M, Oh S-H, Park ED. Direct conversion of cellulose into polyols or H_2 over Pt/Na(H)-ZSM-5. Korean J Chem Eng 2011;28:744–750.

[27] Sotak T, Hronec M, Vavra I, Dobrocka E. Sputtering processed tungsten catalysts for aqueous phase reforming of cellulose. Int J Hydrogen Energy 2016;41:21936–21944.

[28] Zhang J, Yan W, An Z, Song H, He J. Interface-promoted dehydrogenation and water−gas shift toward high-efficient H_2 production from aqueous phase reforming of cellulose. ACS Sustain Chem Eng 2018;6:7313–7324.

[29] Otromke M, Theiss L, Wunsch A, Susdorf A, Aicher T. Selective and controllable purification of monomeric lignin model compounds via aqueous phase reforming. Green Chem 2015;17:3621–3631.

[30] Yan B, Li W, Tao J, Xu N, Li X, Chen G. Hydrogen production by aqueous phase reforming of phenol over Ni/ZSM-5 catalysts. Int J Hydrogen Energy 2017;42:6674–6682.

[31] Li X, Yan B, Znag J, Xu N, Tao Y, Zhang R, Liu B, Sun Z, Chen G. Hydrogen production by aqueous phase reforming of phenol derived from lignin pyrolysis over NiCe/ ZSM-5 catalysts. Int J Hydrogen Energy 2016;42:649-658.

[32] Pipitone G, Tosches D, Bensaid S, Galia A, Pirone R. Valorization of alginate for the production of hydrogen via catalytic aqueous phase reforming. Catal Today 2017; 304:153–164.

[33] Vispute TP, Huber GW. Production of hydrogen, alkanes and polyols by aqueous phase processing of wood-derived pyrolysis oils. Green Chem 2009;11:1433–1445.

[34] Chen A, Chen P, Cao D, Lou H. Aqueous-phase reforming of the low-boiling fraction of bio-oil for hydrogen production: The size effect of Pt/Al_2O_3. Int J Hydrogen Energy 2015;40:14798–14805.

[35] Chen A, Guo H, Song Y, Chen P, Lou H. Recyclable CeO_2–ZrO_2 and CeO_2–TiO_2 mixed oxides based Pt catalyst for aqueous-phase reforming of the low-boiling fraction of bio-oil. Int J Hydrogen Energy 2017; 42: 9577–9588.

[36] Pan C, Chen A, Liu Z, Chen P, Lou H, Zheng X. Aqueous-phase reforming of

the low-boiling fraction of rice husk pyrolyzed bio-oil in the presence of platinum catalyst for hydrogen production. Bioresour Technol 2012;125:335–339.

[37] Seretis A, Tsiakaras P. Crude bio-glycerol aqueous phase reforming and hydrogenolysis over commercial $SiO_2Al_2O_3$ nickel catalyst. Renew Energy 2016;97:373–379.

[38] Boga DA, Liu F, Bruijnincx PCA, Weckhuysen BM. Aqueous-phase reforming of crude glycerol: effect of impurities on hydrogen production. Catal Sci Technol 2015;6:134–143.

[39] Remón J, Giménez JRR, Valiente A, García L, Arauzo J. Production of gaseous and liquid chemicals by aqueous phase reforming of crude glycerol: Influence of operating conditions on the process. Energy Convers Manag 2016;110:90–112.

[40] Kim D, Vardon DR, Murali D, Sharma BK, Strathmann TJ. Valorization of waste lipids through hydrothermal catalytic conversion to liquid hydrocarbon fuels with in situ hydrogen production. ACS Sustain Chem Eng 2016;4:1775–1784.

[41] Swami SM, Chaudhari V, Kim D-S, Sim SJ, Abraham M A. Production of hydrogen from glucose as a biomass simulant: integrated biological and thermochemical approach. Ind Eng Chem Res 2008;47:3645–3651.

[42] Oliveira AS, Baeza JA, Calvo L, Alonso-Morales N, Heras F, Lemus J, Rodriguez JJ, Gilarranz, MA. Exploration of the treatment of fish-canning industry effluents by aqueous-phase reforming using Pt/C catalysts. Environ Sci Water Res Technol 2018; 4; 1979-1987.

[43] Kirilin A V., Hasse B, Tokarev A V., Kustov LM, Baeva GN, Bragina GO, Stakhveev AY, Rautio A-R, Salmi T, Etzold BJM, Mikkola J-P, Murzin DY,

Aqueous-phase reforming of xylitol over Pt/C and Pt/TiC-CDC catalysts: catalyst characterization and catalytic performance. Catal Sci Technol 2014;4:387–401.

[44] Godina LI, Kirilin A V., Tokarev A V., Simakova IL, Murzin DY. Sibunit-supported mono- and bimetallic catalysts used in aqueous-phase reforming of xylitol. Ind Eng Chem Res 2018;57:2050–2067.

[45] Zhu C, Ma Y, Zhou C. Densities and viscosities of sugar alcohol aqueous solutions. J Chem Eng Data 2010;55:3882–3885.

[46] de Miguel SR, Scelza OA, Román-Martínez MC, Salinas-Martínez de Lecea C, Cazorla-Amorós D, Linares-Solano A. States of Pt in Pt/C catalyst precursors after impregnation, drying and reduction steps. Appl Catal A Gen 1998;170:93–103.

[47] Fraga M A., Jordão E, Mendes MJ, Freitas MMA, Faria JL, Figueiredo JL. Properties of carbon-supported platinum catalysts: role of carbon surface sites. J Catal 2002;209:355–364.

[48] Lemus J, Palomar J, Gilarranz MA, Rodriguez JJ. Characterization of Supported Ionic Liquid Phase (SILP) materials prepared from different supports. Adsorption 2011;17:561–571.

[49] de Oliveira GF, de Andrade RS, Concalves Trindade MA, Carvalho Andrade HM, de Carvalho CT, Thermogravimetric and spectroscopic study (TG–DTA/FT–IR) of activated carbon from the renewable biomass source Babassu. Quim Nova 2017;40:284–292.

[50] Schwarz EM, Grundstein VV, Ievins AF. Thermal investigation of polyols I. Hexitols and pentitols. J Therm Anal 1972;4:331–337.

[51] Kumaresan G, Velraj R, Iniyan S. Thermal analysis of D-mannitol for use as

phase change material for latent heat storage. J Appl Sci 2011;11:3044–3048.

[52] Birta N, Doca N, Vlase G, Vlase T. Kinetic of sorbitol decomposition under non-isothermal conditions. J Therm Anal Calorim 2008;92:635–638.

[53] Duarte HA, Sad ME, Apesteguía CR. Bio-hydrogen production by APR of C2-C6 polyols on Pt/Al_2O_3: Dependence of H_2 productivity on metal content. Catal Today 2017;296:59–65.

[54] Duarte HAA, Sad MEE, Apesteguia CRR. Aqueous phase reforming of sorbitol on Pt/Al_2O_3: Effect of metal loading and reaction conditions on H_2 productivity. Int J Hydrogen Energy 2016;41:17290–17296.

[55] Hardman JS, Street PJ. Spontaneous ignition behaviour of TEDA*-carbon. Fuel 1980;59:213–214.

[56] Holade Y, Morais C, Servat K, Napporn TW, Kokoh KB. Enhancing the available specific surface area of carbon supports to boost the electroactivity of nanostructured Pt catalysts. Phys Chem Chem Phys 2014;16:25609–25620.

[57] Guterman VE, Belenov S V, Krikov V V, Vysochina LL, Yohannes W, Tabachkova NY, Tabachkova NY, Balakshina EN. Reasons for the differences in the kinetics of thermal oxidation of the support in Pt/C electrocatalysts. J Phys Chem C 2014:23835–23844.

[58] Sellin R, Clacens JM, Coutanceau C. A thermogravimetric analysis/mass spectroscopy study of the thermal and chemical stability of carbon in the Pt/C catalytic system. Carbon 2010;48:2244–2254.

[59] Baturina OA, Aubuchon SR, Wynne KJ. Thermal stability in air of Pt/C catalysts and PEM fuel cell catalyst layers. Carbon 2006;5:1498–1504.

[60] Mudd JE, Gardner TJ, Sault AG. Platinum catalyzed decomposition of activated carbon: 1. Initial studies, Report. 2001, DOI: 10.2172/791893

[61] Aiouache F, McAleer L, Gan Q, Al-Muhtaseb AH, Ahmad MN. Path lumping kinetic model for aqueous phase reforming of sorbitol. Appl Catal A Gen 2013;466:240–255.

[62] Castoldi MCM, Camara LDT, Aranda DAG. Kinetic modeling of sucrose hydrogenation in the production of sorbitol and mannitol with ruthenium and nickel-Raney catalysts. React Kinet Catal Lett 2009;98:83–89.

[63] Kirilin A V., Tokarev A V., Kustov LM, Salmi T, Mikkola J, Murzin DY. Aqueous phase reforming of xylitol and sorbitol: Comparison and influence of substrate structure. Appl Catal A Gen 2012;435–436:172–180.

[64] Godina LI, Kirilin A V, Tokarev A V, Murzin DY. Aqueous phase reforming of industrially relevant sugar alcohols with different chirality. ACS Catal 2015;5:2989–3005.

[65] Neira D'Angelo MF, Ordomsky V, van der Schaaf J, Schouten JC, Nijhuis TA. Aqueous phase reforming in a microchannel reactor: the effect of mass transfer on hydrogen selectivity. Catal Sci Technol 2013;3:2834–2842.

[66] Neira D'Angelo MF, Ordomsky V, van der Schaaf J, Schouten JC, Nijhuis TA. Continuous hydrogen stripping during aqueous phase reforming of sorbitol in a washcoated microchannel reactor with a Pt–Ru bimetallic catalyst. Int J Hydrogen Energy 2014;39:18069–18076.

[67] Neira D'Angelo MF, Schouten JC, Schaaf J Van Der, Nijhuis TA. Three-phase reactor model for the aqueous phase reforming of ethylene glycol. Ind Eng Chem Res 2014;53:13892–13902.

[68] Huber GW, Shabaker JW, Evans ST, Dumesic JA. Aqueous-phase reforming of ethylene glycol over supported Pt and Pd bimetallic catalysts. Appl Catal B

Environ 2006;62:226–235.

[69] Shabaker JW, Huber GW, Davda RR, Cortright RD, Dumesic JA. Aqueous-phase reforming of ethylene glycol over supported platinum catalysts. Catal Letters 2003;88:1–8.

[70] Wang X, Li N, Webb JA, Pfefferle LD, Haller GL. Effect of surface oxygen containing groups on the catalytic activity of multi-walled carbon nanotube supported Pt catalyst. Appl Catal B Environ 2010;101:21–30.

[71] Wen G, Xu Y, Ma H, Xu Z, Tian Z. Production of hydrogen by aqueous-phase reforming of glycerol. Int J Hydrogen Energy 2008;33:6657–6666.

[72] Wawrzetz A, Peng B, Hrabar A, Jentys A, Lemonidou AA, Lercher JA. Towards understanding the bifunctional hydrodeoxygenation and aqueous phase reforming of glycerol. J Catal 2010;269:411–420.

[73] Bradley KJ, Hamdy MK, Toledo RT. Physicochemical factors affecting ethanol adsorption by activated carbon. Biotechnol Bioeng 1987;29:445–452.

[74] Neira D'Angelo MF, Ordomsky V, Schouten JC, van der Schaaf J, Nijhuis TA. Carbon-coated ceramic membrane reactor for the production of hydrogen by aqueous-phase reforming of sorbitol. ChemSusChem 2014;7:2007–2015.

[75] Kirilin AV, Tokarev AV, Murzina E V, Kustov LM, Mikkola J-P, Murzin DY. Reaction products and transformations of intermediates in the aqueous-phase reforming of sorbitol. ChemSusChem 2010; 3: 708–718.

[76] Neira D'Angelo MF, Ordomsky V, van der Schaaf J, Schouten JC, Nijhuis TA. Selective production of methane from aqueous biocarbohydrate streams over a mixture of platinum and ruthenium catalysts. ChemSusChem 2014;7:627–630.

[77] Sladkovskiy DA, Godina LI, Semikina K V., Sladkovskaya E V., Smirnova DA, Murzin DY. Process design and techno-economical analysis of hydrogen

production by aqueous phase reforming of sorbitol. Chem Eng Res Des 2018;134:104–116.

[78] indexmundi.com, accessed 27. 02.2019